ACS OMEGA

Open Access

http://pubs.acs.org/journal/acsodf

Article

Bioengineered Injectable Hydrogel Based on the Dentin Extracellular Matrix and Chitosan

Sajdah Arbeed, Maya Osman, Feng Gao, Stephen Suchy, Zinat Sharmin, Joshua Z. Gasiorowski, Amber Kaminski, Ira M. Sigar, and Marcela R. Carrilho*

Cite This: *ACS Omega* 2025, 10, 9210–9223

Read Online

ACCESS | Metrics & More | Article Recommendations

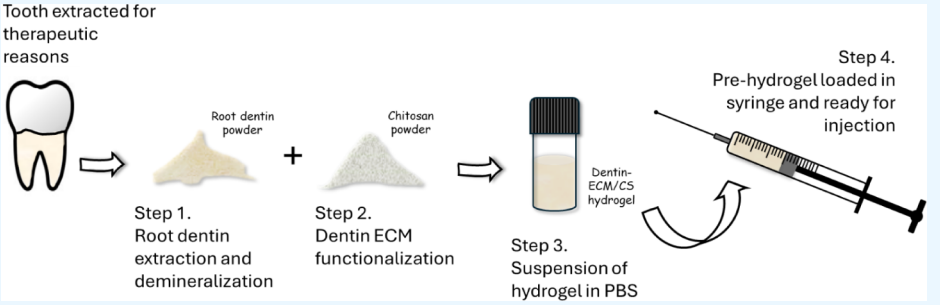

ABSTRACT: The extracellular matrix of dentin contains macromolecules of biological value that make it a natural source for the prospection of novel smart biomaterials. Here, we described the development of an injectable thermosensitive smart hydrogel resulting from the blending of insoluble macromolecules of the dentin matrix and chitosan. The extrudability and gelation parameters of the prehydrogel were optimized by varying the concentration of individual components. Three-dimensional constructs were fabricated upon injection of the prehydrogel into custom-made molds, followed by incubation at 37 °C. Specimens were characterized for spectral, physical, morphological, mechanical, and biocompatibility features. Fourier-transform infrared (FTIR) analyses confirmed the integration of the dentin organic matrix and chitosan. The degree of porosity of constructs was ∼51%. The water diffusion of constructs reached a plateau after 2 days. Their moduli of elasticity were at a low MPa order, decreasing after storage in simulated body fluid (SBF). The biodegradability of constructs rose following incubation in SBF containing lysozyme or zinc ions. Hydrogel bioactivity was confirmed by FTIR and ultramorphologically suggested by surface precipitates. Hydrogel constructs were shown to be biocompatible with undifferentiated pulp cells (OD-21). Overall, the novel engineered injectable hydrogel based on dentin extracellular macromolecules and chitosan holds promising features for use as a scaffold for the regeneration of damaged load-bearing tissues like dentin and bone.

1. INTRODUCTION

The integral and endogenous repair of load-bearing mineralized tissues (i.e., bone, enamel, dentin, cementum) imposes a substantial constraint on the progress of regenerative therapies in dentistry and medicine.[1] Part of this challenge is related to the lack of adequate biofabrication strategies and biomaterials that are capable of reproducing the intricate compositional and architectural characteristics that are unique to these substrates.[2] Biomaterials designed for three-dimensional (3D) bioprinting (i.e., bioinks) and/or in situ delivery emerge as technologies with the potential to address this critical gap in the regeneration of load-bearing tissues. As bioinks are extrudable biomaterials, they enable the controlled placement of self-assembled cell structures on demand, therefore offering convenient means for bioengineering critical-sized defects in these tissues.[3,4]

The crucial role of extracellular matrices (ECMs) in tissue/organ development and function is well established,[5] but their value in tissue re-engineering and de novo development has gained special attention only more recently.[6] Tissue ECMs are reservoirs of bioactive molecules and biophysical cues,[7] which can increase scaffold productivity and effectiveness.[8] Accordingly, the decellularized ECM of native tissues can be conveniently utilized as a natural raw biomaterial for the design of injectable biomaterials, bioinks, and scaffolds for tissue bioengineering.[9,10]

The ECM that has yet to be explored as a resource to produce scaffolds for use in tissue engineering is that of dentin. Dentin is the mineralized connective hard tissue constituting the core and

Received: October 15, 2024
Revised: January 28, 2025
Accepted: February 4, 2025
Published: February 25, 2025

most abundant structure of all teeth.[11] The presence of a densely collagen-packed, acellular, and avascular organic matrix in mature dentin represents an opportune model to explore the inductive function of biological scaffolds in the reconstruction of injured tissues.[12] Dentin, namely its ECM, can be easily acquired as a biological product of the therapeutic extraction of a tooth (i.e., as required by orthodontic and periodontal therapy) and serve in the design of bioinspired engineered materials.[10,13]

Chitosan is a naturally occurring polysaccharide with chemical and biological properties that resemble those of glycosaminoglycans, ubiquitous macromolecules of the ECMs of load-bearing tissues.[12] Chitosan and chitosan-based biomaterials have been shown to exhibit a number of invaluable biological attributes, including antifungal, antibacterial, analgesic, mucoadhesive, and anti-inflammatory properties, as well as high versatility for chemical functionalization.[14−16] Nonetheless, chitosan has very low solubility in most organic solvents, including water, which impairs its application in tissue engineering schemes if modifications are not properly made to accommodate this limitation.

Herein, we describe the synthesis and characterization of a novel biomaterial that takes advantage of the biological functionalities of chitosan to blend them with those of a unique load-bearing structure of the tooth, the ECM of dentin. We and others have shown that the ECM of dentin comprises a pool of bioactive molecules and macromolecules with high odontogenic/osteogenic differentiation potential.[17−20] The newly engineered hydrogel was optimized to conform with injectable and thermosensitive features for primary application in dental tissue regeneration, with potential for translation to other biomedical applications where the use of ECM-derivative hydrogels is key to support in situ tissue regeneration of load-bearing tissues, such as bone and cartilage. We hypothesized that this new biomaterial would exhibit intrinsic properties to assist therapies aimed at promoting the endogenous regeneration of the injured dentin-pulp complex.

2. MATERIALS AND METHODS

Chemicals and reagents used in this study were purchased from Fisher Scientific (Hampton, NH, USA) or Sigma-Aldrich (St. Louis, MO, USA), unless otherwise specified.

Sixty-five extracted noncarious human third molars and second premolars, which would otherwise be discarded, were collected from oral surgery and dental implant centers in the Chicago area. Since no data or identifiers on tooth donors were available and/or traceable by any investigator, the Institutional Review Board of Midwestern University-DG determined that this study was not human subjects research. The collected teeth were maintained in saline containing 0.02% NaN_3 at −20 °C and used up to 6 months after collection.

2.1. Extraction of the Dentin Extracellular Matrix. The root and crown portions of selected teeth were separated using a slow-speed diamond saw (Labcut 150, Extec, Enfield, CT, USA). Only root dentin fragments were used for the synthesis of the proposed biomaterial. The cementum surrounding each dental root fragment was fully removed using a diamond bur mounted in a dental handpiece, while the pulp tissue was extirpated with endodontic files (Lexicon presterilized K-file 21 mm, Dentsply Sirona, Charlotte, NC, USA). Small fragments of root dentin (~4 mm^2) were thoroughly rinsed with water, stored in absolute ethanol for 30 min, and immersed in liquid nitrogen for 30 min to be subsequently ground into powder using a ball mill (MM200, Retsch, Newtown, PA, USA) for 7 min at 25 Hz. The powdered dentin was sieved twice through a series of ASTM E11 certified sieves with descending pore sizes #24 (710 μm), #40 (425 μm), #70 (212 μm), and #140 (106 μm) (Fisherbrand, Waltham, MA, USA) to obtain particles with a size of <106 μm.

2.2. Demineralization of the Dentin ECM. The powdered dentin sample was demineralized by using acetic acid. Samples were split into 1-g aliquots, which were then added to 10 mL of 1 M acetic acid. They were maintained in sealed tubes under agitation at 4 °C for 7 days to ensure that the dentin ECM was sufficiently demineralized. The acetic acid of each sample was replaced 3 times during the 7-day period of dentin demineralization. Acetic acid-treated dentin powder, from now on referred to as demineralized dentin ECM, was centrifuged (3200 *g*, 4 °C) and dialyzed against ultrapure water for 4 days, subsequently air-dried overnight at room temperature, lyophilized, weighed, and stored at −80 °C until use.

2.3. Functionalization of the Dentin ECM with Chitosan. The freeze-dried demineralized dentin ECM powder was resuspended in 0.1 M precooled acetic acid (pH 5.2, 20 mg/mL; suspension A). Low molecular weight chitosan (CAS# 9012−76−4, Product# 448869, MW: ~50 000−190 000 Da depending on final viscosity) was dissolved in 0.02 M of precooled acetic acid to obtain a 2 wt/v% chitosan suspension with pH 6 (suspension B). Suspensions A (demineralized dentin ECM) and B (chitosan) were mixed in a volume ratio of 25:75 and allowed to degas for 24 h.[21] The rationale for choosing this dentin ECM/Chitosan volume ratio is based on a previous study[21] that developed injectable collagen/chitosan hydrogels using exactly this ratio, i.e., 25 v/v% dentin ECM/75 v/v% chitosan. Since the most abundant protein in the dentin ECM is type I collagen[11] (over 90% by weight), we reasoned that this would be a suitable volume ratio to start with for what we believe is the first attempt to create a hydrogel combining chitosan with the dentin ECM. Precooled β-glycerophosphate (BGP) sodium salt was added to the mixture of suspensions A and B as the cross-linking agent to a final concentration of 5.8 wt/v%. BGP sodium salt is often used as an initiator for thermosensitive sol−gel transition of chitosan-collagen hydrogel precursors because it increases the solubility of chitosan-collagen solution and changes its gelation temperature to 37 °C without the need for any further chemical cross-linking.[22,23] All syntheses were carried out on ice to maintain the material in a liquid state. The resultant mixture was separated into 2-mL aliquots, freeze-dried for 4 days (VirTis, SP Scientific, Warminster, PA, USA), and stored at −20 °C until use.

2.4. Degree of Extrudability/Injectability, Gelation, and Infrared Spectral Features of the Dentin ECM/Chitosan Prehydrogel. The dentin ECM/Chitosan hybrid material, which presented a spongy appearance after lyophilization, was resuspended in physiological buffer (PBS) at a concentration of 100 mg/mL and will henceforth be called prehydrogel. Twenty microliters of 1 N sodium hydroxide were added per milliliter of prehydrogel to adjust its pH to a physiological value (7.3). The extrudability of the prehydrogel was assessed at different temperatures ranging from 4 to 37 °C using both P-20 and P-1000 pipettes.[24]

Additionally, the injectability of the prehydrogel was investigated by an injection force model using a 1 mL syringe and a 27-gauge needle, modified from prior studies.[25,26] The syringe was loaded with the cooled dentin ECM/Chitosan prehydrogel and equilibrated at a controlled room temperature (23 ± 3 °C) and relative humidity (~65%) for 30 min before

https://doi.org/10.1021/acsomega.4c09413
ACS Omega 2025, 10, 9210−9223

starting measurements. Injection force evaluation was performed using a universal testing machine (Shimadzu, EZ-LX, Columbia, MD, USA) and a 500 N load cell at a speed of 1.0 mm/min. The hydrogel was expelled by pushing the syringe plunger at a constant speed and injecting 1.0 mL of the prefilled volume of a 10 mm long syringe onto a Petri dish in 10 s.[25,26] The contraction force was measured as a function of distance, and the maximum force at the plateau of the force−displacement distance graph was arbitrarily represented by the sliding force at the end of the injection. The syringe's inner diameter and needle length were measured with a digital caliper (Mitutoyo, Chicago, IL) and used for the calculation of the friction force using the Hagen−Poiseuille law, and compared with the injection force of a similar syringe filled with water, which was chosen as a control for Newtonian behavior.[26] The final injection force comprises the hydrodynamic force and the friction force, which in turn represents the sliding friction and considers the contribution of the compression of the plunger that is in equilibrium at the sliding force plateau.[25] The experiments were repeated 3 times for consistency.

The gelation kinetics of the hydrogel were evaluated by the tube inversion method. 1 mL samples of the precooled prehydrogel (n = 5) were transferred to test tubes and placed in a water bath set at 20 °C. The bath temperature was progressively increased to 37 °C. The flowability of the samples was observed every 10 s by tilting the tube.[27] The time and temperature at which the hydrogel flow stopped were recorded as the coordinates of the gelation point.

Infrared spectroscopy (FTIR) analysis[28] of the hydrogel precursor was conducted using the ATR-FTIR Spectrum Two (PerkinElmer, Waltham, MA, USA). To ensure optimal contact, samples were slightly clamped against the ATR crystal by using a standardized gauge force. The ATR-FTIR analysis parameters were set in the mid-infrared region (4000 to 400 cm^{-1}), and spectra were collected with an average of 512 scans at 4 cm^{-1} spectral resolution. ATR-FTIR spectra were also acquired for demineralized dentin ECM, chitosan, and BGP. All collected spectra were background-corrected and normalized with a Savitzky-Golay filter. These experiments were performed in triplicate to ensure accuracy.

2.5. Sol−Gel Fraction Analysis of Dentin ECM/Chitosan Constructs. 3D disk-like constructs of dentin ECM/Chitosan hydrogels were used to perform the sol−gel analysis. This assessment determines the concentration of the unreacted monomer (sol) and polymer (gel) in the fabricated hydrogel system.[28] First, the prehydrogel was lyophilized to obtain a sponge-like material that was subsequently resuspended in PBS (50 mg/mL) and left rotating at a slow speed at 4 °C overnight. Subsequently, disc-like 3D specimens (n = 7) were prepared by injection of the resuspended dentin ECM/Chitosan prehydrogel at ∼20 °C into custom-made molds (diameter = 3.5 mm; thickness = 1.5 mm) using a P-20 pipette. After gelation (i.e., 10 min incubation at 37 °C), the specimens were freeze-dried, weighed (Ma) (ML104T/00, Mettler Toledo, Columbus, OH, USA), and placed in boiling water (∼100 °C) for approximately 4 h. Next, they were taken out from the water bath, placed in a desiccator at 37 °C for 8 h, and weighed again (Mb). The sol and gel fractions of hydrogel constructs were calculated by using the following formulas: (1) gel fraction (%) = [(Mb/Ma) × 100] and (2) sol fraction (%) = (100 − gel fraction) [where: Ma is the mass of the construct after freeze-drying and Mb is the hydrogel desiccated mass following hot water extraction for 4 h].[28]

2.6. Degree of Porosity of Dentin ECM/Chitosan Constructs. The degree of porosity within the hydrogels was evaluated using a liquid displacement method.[21] Disc-like specimens (n = 5), prepared as previously described in Section 2.5, were freeze-dried and had their initial mass (W_1) and volume (V_1) measured and recorded. The constructs were immersed in ethanol (EtOH) at room temperature (22 ± 3 °C) for 24 h, during which they were expected to be fully saturated. After being gently blot-dried, the mass (W_2) and volume (V_2) of the constructs were measured again.[21] The degree of porosity was calculated using the equation: porosity (%) = $[(W_2 - W_1)/(V_2 - V_1) \times (D_{EtOH})] \times 100$ [where D_{EtOH} is the density of ethanol, which is 0.789 g/mL at 25 °C].

2.7. Scanning Electron Microscopy (SEM) Analysis of Dentin ECM/Chitosan Constructs. The morphology and pore structure of hydrogel disc-like constructs were prepared as described in Section 2.5 and were evaluated using scanning electron microscopy (JCM-6000 Plus, JEOL, Peabody, MA, USA).[21,29] Before analysis, the specimens (n = 3/group) were dried by different methods: 1) air-drying (i.e., at room temperature for 24 h); 2) chemical-drying (i.e., critical point dryer, CPD300, Leica EM, Teaneck, NJ, USA); 3) freeze-drying (VirTis, SP Scientific). Samples were then sputter-coated with silver and evaluated under a 10 kV electric current (ACE600, Leica EM).

2.8. Water Sorption, Solubility, and Degree of Swelling of Dentin ECM/Chitosan Constructs. Twenty-one freeze-dried disc-like constructs of the dentin ECM/Chitosan hydrogel were prepared as described in Section 2.5. The specimens were weighed using an analytical balance to obtain the initial dry mass (m_1). The diameter and thickness of dried constructs were measured using a digital caliper (rounded to the nearest 0.01 mm). These measurements were used to calculate the volume (V) of each specimen (in mm^3). The constructs were individually placed in sealed glass vials containing 1 mL of ultrapure water (pH 7.2) supplemented with 0.02% NaN_3 and stored at 37 °C for 2, 8, or 16 days (n = 7 specimens/storage time). At each endpoint, the specimens were gently washed in running water, blot-dried with a soft absorbent paper, weighed to assess their wet mass (m_2) and left to dry inside a desiccator until a constant final dry mass (m_3) was obtained. The water sorption (WS), solubility (SL), and degree of swelling (DS) were calculated using the following formulas: $WS = (m_2 - m_3)/V$, $SL = (m_1 - m_3)/V$ and $DS\% = [(m_2 - m_1)/m_1]/V$. Data of WS, SL, and DS were individually analyzed by one-way ANOVA and Tukey post hoc tests (α = 0.05).

2.9. Flexural Modulus of Elasticity of Dentin ECM/Chitosan Constructs. Three-point bending tests were used to measure the flexural moduli of elasticity (E) of hydrogel constructs by a nondestructive approach, using a 5 N load cell mounted on a universal testing machine (EZ-LX, Shimadzu) and a customized two-point sample holder with a support span of 2.5 mm. Sixty bar-like specimens were prepared by injecting the dentin ECM/Chitosan PBS-resuspended hydrogel into custom-made molds (1.5 × 1.5 × 10 mm) at 20 °C using a P-20 pipette. After gelation (i.e., 10 min incubation at 37 °C), the specimens were kept in a desiccator for 12 h, weighed for obtaining their initial dry mass, and rehydrated in ultrapure water for 6 h at 37 °C. They were then placed at rest in the sample holder, previously filled with water, and equilibrated at controlled room temperature (23 ± 3 °C) and relative humidity (65%) for 10 min before starting the measurements. This protocol was defined in a pilot study and aimed to standardize

https://doi.org/10.1021/acsomega.4c09413
ACS Omega 2025, 10, 9210−9223

the humidity level of the specimens and minimize its impact on the variation of the flexural elastic modulus. Specimens were individually loaded at a crosshead speed of 0.5 mm/min to a 5% strain to obtain specimens' initial (baseline) flexural E. The E values were calculated as the steepest slope of the linear portion of the load−displacement curve using the formula: $E = L^3F/4wT^3d$, where L is the span length of sample support (mm), F is the applied force (load) (N), w is the width (mm) of test specimens, T (mm) is their thickness, and d is the deflection (mm). The E (N/mm^2) values were expressed in MPa.

Afterward, specimens were divided into two equal sets of samples and incubated in 1 mL of simulated body fluid [SBF= 0.14 M NaCl, 4 mM $NaHCO_3$, 3 mM KCl, 8 mM $K_2HPO_4 \cdot 3H_2O$, 1.5 mM $MgCl_2 \cdot 6H_2O$, 40 mM HCl, 2.6 mM $CaCl_2$, 0.5 mM Na_2SO_4, 3 mM NaN_3, and 50 mM Tris-HCl][30] daily spiked with either 2 μg/mL of lysozyme (SBF+LYS)[29] or 1 mM $ZnCl_2$ (SBF+Zn).[31] The rationale to supplement samples' storage media with lysozyme or Zn was to challenge the specimen degradability, primarily through the chitosan, by cleavage of its 1,4-beta-linkages between *N*-acetylmuramic acid and *N*-acetyl-D-glucosamine mediated by lysozyme,[32] or by hydrolysis of dentin collagen mediated by matrix metalloproteases, whose activity depends on the presence of Zn and Ca.[33] Samples were stored individually in each of the SBF media (pH 7.4) and incubated at 37 °C under constant agitation for 2, 8, or 16 days (n = 10 specimens/SBF media/storage time). At each endpoint, the specimens were washed in running water and had their final flexural E assessed again as described. Differences between initial and final flexural E values for each storage medium (i.e., SBF +LYS or SBF+Zn) were calculated and separately analyzed by two-way repeated ANOVA and Tukey post hoc tests (α = 0.05). Comparisons between SBF media were performed individually for each storage time (i.e., 2, 8, and 16 days) and analyzed by two-way ANOVA and Tukey post hoc tests (α = 0.05).

2.10. Biodegradability of Dentin ECM/Chitosan Constructs. Two biodegradability analyses were run using samples prepared for E evaluation; one assessed the changes in specimens' mass by gravimetry[29] and the other evaluated the amount of collagen degradation in SBF+n by assessment of its unique residue, hydroxyproline.[31] For the gravimetric tests, the beam-like constructs that were stored either in SBF+YS or SBF +Zn were dried in an incubator at 37 °C for 12 h and weighed to obtain a dry mass after SBF storage (dry mass after SBF). The biodegradation rate indicated by changes in the dry mass of beam-like specimens before ($Dry\_mass_{\_baseline}$) and after ($Dry\_mass_{\_after\ storage}$) SBF incubation for each storage medium was calculated by the equation: biodegradation rate (%) = $[(Dry\_mass_{\_baseline} - Dry\_mass_{\_after\ storage})/Dry\_mass_{\_baseline}] \times 100$. Data concerning each SBF medium were separately analyzed by ANOVA two-way repeated measures and Tukey post hoc tests (α = 0.05).

For the hydroxyproline (HYP) assay, at each time point (2, 8, and 16 days), the incubation medium SBF+Zn used to store each specimen was retrieved and freeze-dried. The basis for assessing the collagen degradation by the HYP assay lies in the fact that type I collagen, which comprises ≈90% (mass) of the dentin matrix, contains a distinguished concentration of HYP of about 10 wt %. Therefore, the absorbance of HYP observed in the incubation medium can be used to estimate the degree of solubilized dentin ECM collagen via endogenous proteases.[33] Absorbance values were measured spectrophotometrically (DS-11 FX+, DeNovix, Inc., Wilmington, DE, USA) at 550 nm against standard curves of known concentrations of HYP (2 to 20 μg/mL). The solubilized collagen was expressed as micrograms of HYP per milligram of specimen baseline dry mass (μg of HYP/mg of specimen dry mass). Data were analyzed by one-way ANOVA and Tukey post hoc tests for multiple comparisons (α = 0.05).

2.11. In vitro Bioactivity of Dentin ECM/Chitosan Constructs. Fifteen new disc-like constructs of the hydrogel were prepared as described in Section 2.5. The specimens were freeze-dried and individually placed in sealed glass vials containing 1 mL of simulated body fluid (bioact-SBF)* that has been shown to be stable relative to changes in ion concentrations with storage period and with optimum ion concentrations for in vitro bioactivity assessment of biomaterials and biomimetic production of bone-like apatite[30,34] *(i.e., bioact-SBF = 92 mM NaCl, 6 mM $NaHCO_3$, 4 mM Na_2CO_3, 3 mM KCl, 8 mM $K_2HPO_4 \cdot 3H_2O$, 1.5 mM $MgCl_2 \cdot 6H_2O$, 35 mM NaOH, 75 mM HEPES, 2.6 mM $CaCl_2$, 0.5 mM Na_2SO_4, and 3 mM NaN_3, pH 7.4). Samples were incubated at 37 °C under constant agitation for 2, 8, or 16 days (n = 5 specimens/bioact-SBF media). At each endpoint, the specimens were washed in running water and air-dried at 37 °C overnight. Three specimens were analyzed by using ATR-FTIR to check the potential increase in IR spectral bands/peaks corresponding to apatite (i.e., 564, 938, and/or 1000 cm^{-1}) after incubation in bioact-SBF.[20] The remaining specimens were prepared for SEM analysis for the identification of precipitate/deposit formation on the dentin ECM/Chitosan surface. Briefly, at each endpoint, specimens were removed from bioact-SBF, placed in a desiccator overnight, sputter-coated with silver (ACE600, Leica EM), and analyzed under 10 kV.

2.12. Biocompatibility of Dentin ECM/Chitosan Constructs. The PBS-suspended prehydrogel was directly injected into wells of a 96-well plate and freeze-dried for 8 h to form constructs approximately 1.5 mm thick. Specimens of hydraulic calcium silicate cement (EndoSequence BC Sealer, Brasseler US Dental Instrumentation, Savannah, GA, USA) were used as a reference benchmark biomaterial routinely used to assist the repair of the dentin-pulp complex and dental root apex. The plate was incubated at 37 °C for 30 min and then exposed to ultraviolet light for 10 min for sample sterilization. The murine undifferentiated pulp cells OD-21 were seeded onto each construct at a density of 2.5 × 10^3. The control group consisted of OD-21 cells seeded on polystyrene-coated wells. Samples and respective blank wells were supplemented with regular cell culture media containing DMEM (with fetal bovine serum) and stored in a 37 °C and 5% CO_2 incubator. Assessment of OD-21 cells' metabolic activity was performed using the alamarBlue assay in three (n = 3) independent experiments. The absorbance of the samples was measured at 570 nm. Cell viability on tested materials (dentin ECM/Chitosan × calcium silicate) was expressed as a percentage of the control group, which was considered to exhibit the maximum cell viability (100%). Data did not fit into a normal distribution and were analyzed by nonparametric tests (Kruskal−Wallis and post hoc Dunn's test).

Furthermore, OD-21 cells were evaluated by the LIVE/DEAD Viability/Cytotoxicity kit (Invitrogen, Waltham, MA, USA), which discriminates between live and dead cells by simultaneous staining, where green-fluorescent calcein-AM indicates intracellular esterase activity (live cells) and red-fluorescent ethidium homodimer-1 indicates a loss of plasma membrane integrity (dead cells). For this, OD-21 cells were seeded onto hydrogel cast on 48-well plates at a density of 1 × 10^5 and supplemented with regular cell culture media containing

https://doi.org/10.1021/acsomega.4c09413
ACS Omega 2025, 10, 9210−9223

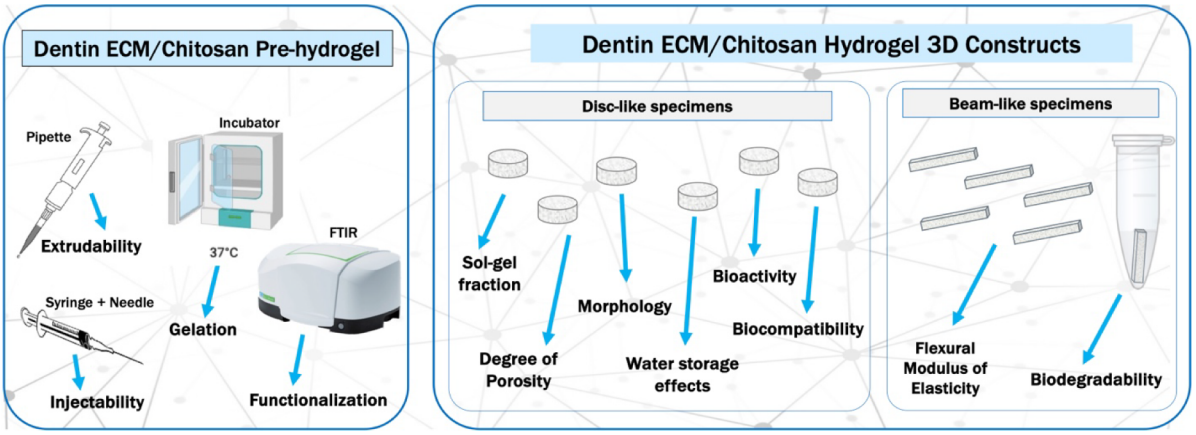

Figure 1. Illustration of characterization of ECM/Chitosan prehydrogel and hydrogel constructs..

DMEM (with fetal bovine serum) and stored at 37 °C in a 5% CO_2 incubator. The metabolic activity of OD-21 cells was spectrophotometrically measured (Promega GloMax Plate Reader, Madison, WI, USA; with excitation λ = 475 nm and emission λ = 525 nm) and imaged under a fluorescence microscope (Nikon Eclipse Ti2-E, Melville, NY, USA). All measurements were repeated 3 times. The viability of OD-21 cells assessed by the spectrophotometer was expressed as a percentage of the control group (OD-21 cells seeded in untreated wells), which was considered to be maximal (i.e., 100% cell viability). Since these data fit a normal distribution, they were analyzed by parametric tests (ANOVA and Tukey post hoc). Figure 1 summarizes the study's experimental design.

3. RESULTS

Each experiment/material characterization was repeated at least 3 times to ensure data reliability. Low molecular chitosan was used to functionalize the dentin ECM obtained from different pools of teeth and, therefore, from different batches of demineralized dentin. By the characterization of resultant prehydrogels and hydrogel constructs, it was found that differences among different batches of the dentin ECM were not significantly greater (or lower) than those observed within a single batch. Thus, regardless of the intrinsic variability between dentin substrates extracted from different teeth, the functionalization of the dentin ECM by chitosan was shown to be fairly reproducible and consistent.

3.1. Degree of Extrudability/Injectability, Gelation, and Infrared Spectral Features. The prehydrogel was shown to be extrudable using P-20 and P-1000 pipettes at temperatures ranging from 4° to 25 °C (Figure 2a). The extrudability of the prehydrogel was also indirectly evaluated as a result of the fabrication of 3D constructs obtained after its injection into custom molds and incubation at 37 °C for ∼10 min (Figure 2a).

The injection force, also known as hydrodynamic force, was calculated using the Hagen−Poiseuille equation (Figure 2b) with an injection rate of 1.0 mL/10 s, as commonly used for injectability testing.[25,26] The measurements of the injection force × injection speed and the shear rate of prefilled syringes with the prehydrogel were plotted against controls (water) and indicated a slight deviation from the Newtonian fluid model (Figure 2b).

The gelation of the developed material was obtained after pH adjustment to neutral (∼7.3) and incubation at 37 °C for 10 (±2) minutes. Although the viscosity of this thermosensitive prehydrogel has not been directly measured by the rheometric approach, a progressive increase of its viscosity was noticed as the temperature rose. This phase transition was visually assessed by inverting the tubes containing the hydrogel at different temperatures (Figure 2c). Additionally, because the behavior of the prehydrogel deviates slightly from a Newtonian fluid, as measured by the injection force modeling, its viscosity was estimated by the Hagen−Poiseuille equation (Figure 2b).

FTIR spectral analysis confirmed the functionalization of the dentin ECM by chitosan (Figure 2d). The dentin ECM/Chitosan prehydrogel spectrum was plotted along with the spectra of pristine components: chitosan, cross-linking agent BGP, and the demineralized dentin ECM. Representative IR peaks for these compounds and the derived hydrogel, as seen in Figure 2d, were at the following wavenumbers (cm^{-1}):

- Chitosan: ∼3361−3000 (−OH stretching and −NH stretching of amide A), at ∼2920 (−CH symmetric stretching), ∼2877 (−CH asymmetric stretching), ∼1645 cm^{-1} (—C═O stretching of amide I), ∼1423 (−CH2 bending), ∼1375 (−CH3 symmetrical), ∼1325 (−C−N stretching of amide III), ∼1260 (−OH bending), ∼1153 (−C−O−C bridge asymmetric stretching), ∼1066 (−C−O stretching), and ∼896 (−CH bending);
- BGP: ∼3330−3290 (−OH stretching of water), ∼1664 (C═O stretching of amide I), ∼1457 (—C═O stretching), ∼1112 (O−O stretching), ∼1080 (C−O stretching), ∼1069 (C−O−C stretching vibrations), ∼912 (═C—H bending), ∼779 (═C—H bending), and ∼645 (O−H bending);
- Demineralized dentin ECM: ∼3330−3290 (−NH stretching of amide A), ∼1640 (—C═O stretching of amide I), ∼1550 (−NH bending of amide II), ∼1450 (−CH2 scissoring of CH), ∼1241 (C−N stretching and N−H bending of amide III), ∼1153 (−C−O−C bridge asymmetric stretching), ∼1046 (═P—O stretching of PO_4^3), ∼871 (−CH bending), ∼770 (═C—H bending), ∼660 (O−H bending), and ∼567 (═P—O stretching of PO_4^3);
- Dentin ECM-CS hydrogel: ∼3560−3000 (−NH stretching of amide A), ∼1658 (C═O stretching of amide I), ∼1571 (−NH bending of amide II), ∼1411 (C−H bending), ∼1190 (−C−O−C bridge asymmetric stretching), ∼1080−1060 (overlapping of C−O stretching, C−O−C stretching and −NH bending), at ∼978 (═P—O

https://doi.org/10.1021/acsomega.4c09413
ACS Omega 2025, 10, 9210−9223

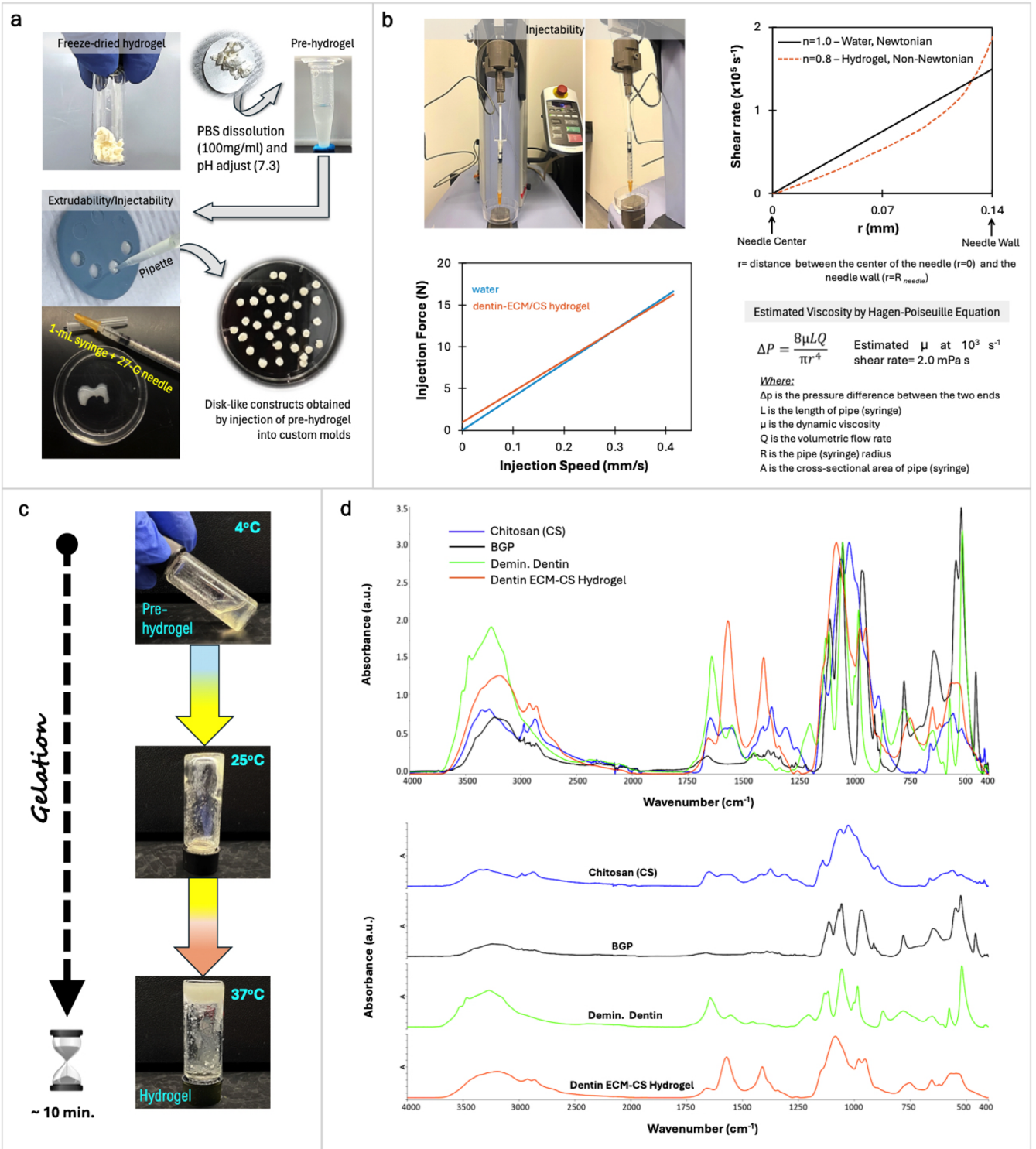

Figure 2. (a) Extrudability of the prehydrogel with P-20 and P-1000 pipettes and syringe + 27-gauge needle; (b) injectability, estimated viscosity, and shear rate of the prehydrogel using prefilled syringes and 27-gauge needles, and having water as control of a Newtonian fluid; (c) gelation assessed by a tube tilting method, showing change in the prehydrogel viscosity as a function of temperature increase; (d) ATR-FTIR-spectrum of the functionalized dentin ECM/Chitosan hydrogel (orange line) against spectra of pristine components, demineralized dentin (bright green line), chitosan (blue line), and BGP (black line). All experiments were repeated 3 times to ensure accuracy.

stretching of PO_4^3), ~951 (=C—H bending), ~750 (=C—H bending), ~652 (O—H bending), and ~650–500 (=P—O stretching of PO_4^3 (ν_3) and PO_4^3 (ν_4)).

The permanence of most of these characteristic IR peaks/bands in the newly synthesized dentin ECM/CS hydrogel indicates that the integration of the dentin ECM and chitosan did not affect these compounds' baseline structures. Furthermore, shifts in the absorbance and wavenumber of some of those characteristic peaks and bands confirmed that BGP effectively mediated the interaction between the dentin ECM and chitosan.

https://doi.org/10.1021/acsomega.4c09413
ACS Omega 2025, 10, 9210−9223

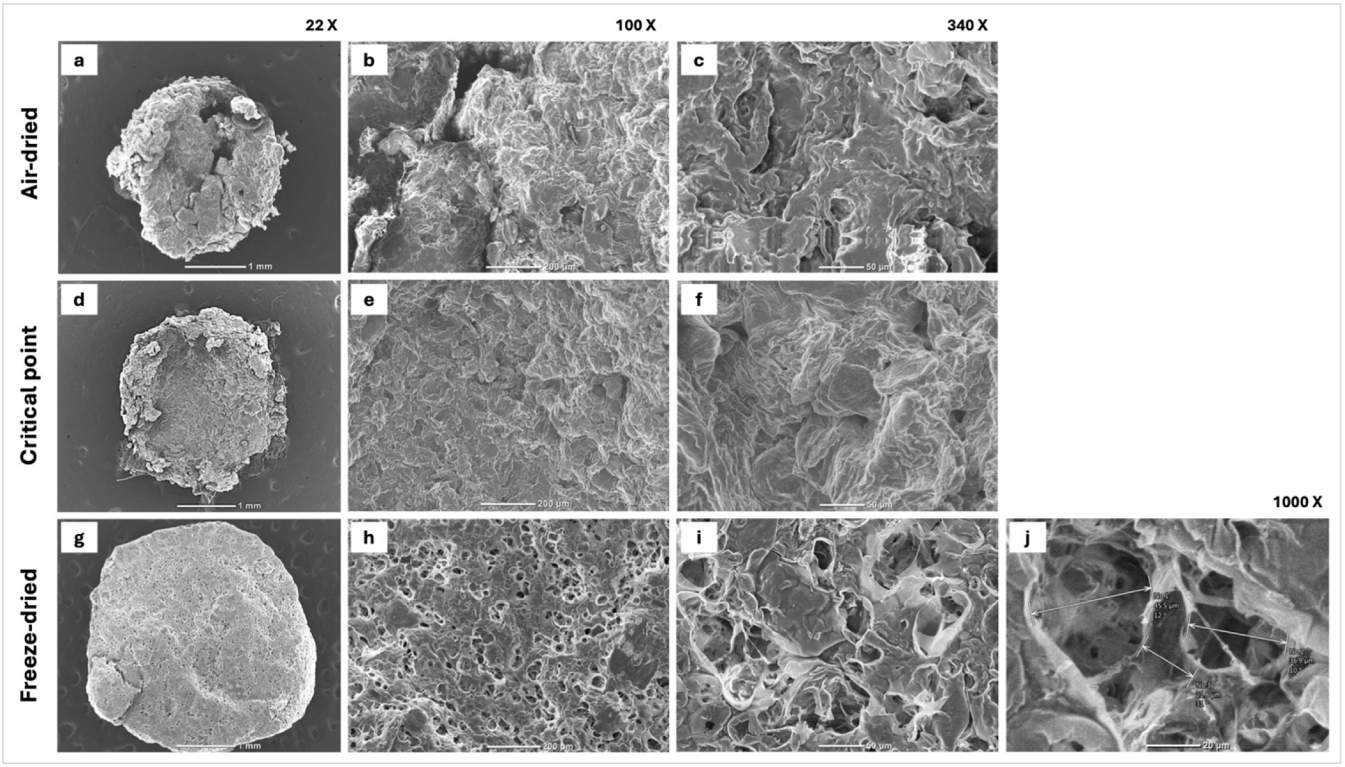

Figure 3. SEM analysis of morphology and porosity features in representative specimens of the dentin ECM−Chitosan hydrogel at magnifications of 22× (bar = 1 mm), 100× (bar = 200 μm), 340× (bar = 50 μm), and 1000× (bar = 20 μm). (a-−c) Air-dried 3D construct at 22×, 100×, and 340×; (d-−f) critical point chemical-dried 3D construct at 22×, 100×, and 340× magnification; (g-−j) freeze-dried (lyophilized) 3D construct at 22×, 100×, 340×, and 1000× magnification.

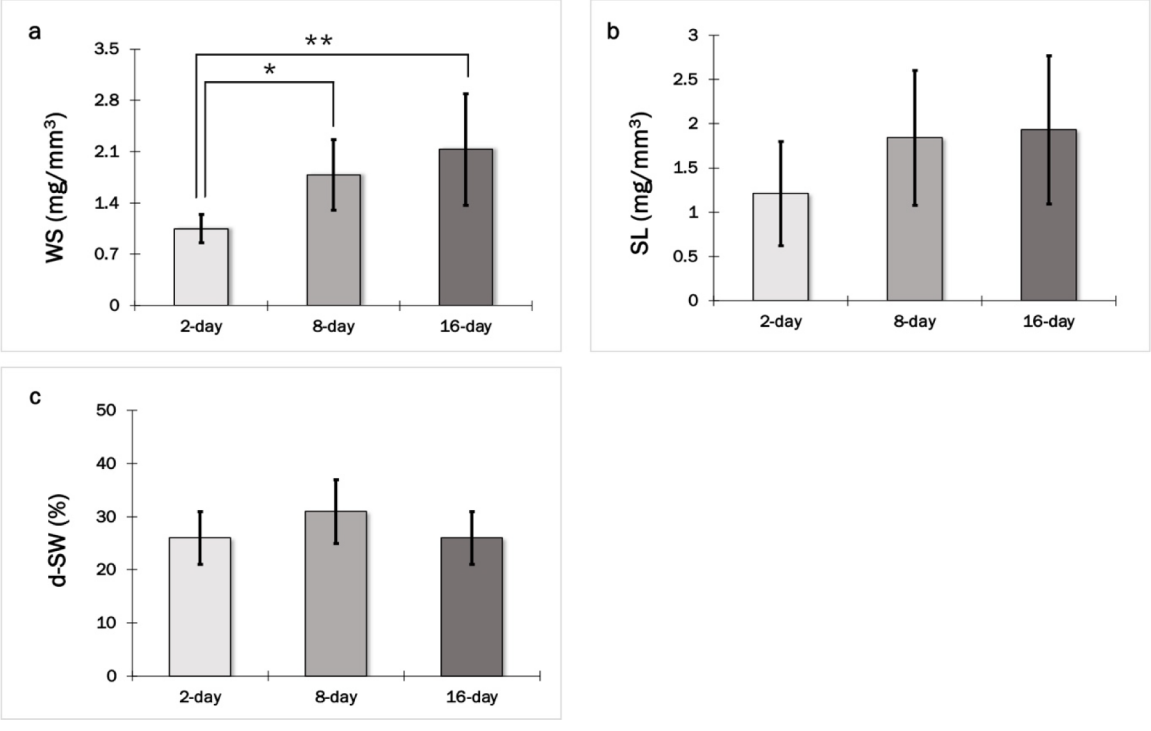

Figure 4. Water sorption (WS), solubility (SL) and degree of swelling (d-SW) in constructs of the dentin ECM−Chitosan hydrogel following storage in water for 2, 8, or 16 days. Values are presented as mean ± SD (n = 7 specimens/storage time). (a) Differences in WS values were statistically significant between 2- and 8-day storage (*p = 0.01) and between 2- and 16-day storage (**p = 0.002); (b) SL and (c) d-SW values did not differ significantly between the tested endpoints.

https://doi.org/10.1021/acsomega.4c09413
ACS Omega 2025, 10, 9210−9223

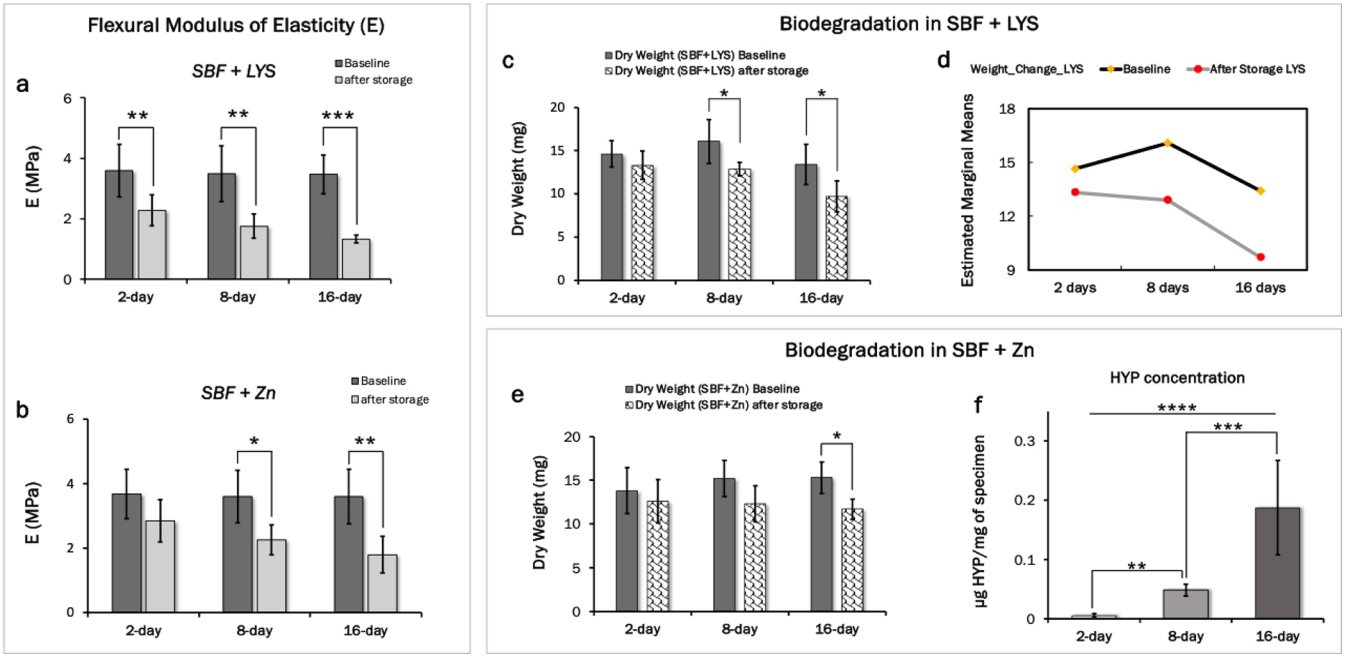

Figure 5. Effects of SBF+LYS and SBF+Zn on the dentin ECM−Chitosan hydrogel modulus of elasticity (AE) and biodegradation rate. (a) Changes in E (MPa) for constructs stored in SBF+LYS (values are presented as mean ± SD, n = 10); (b) changes in E (MPa) for constructs stored in SBF+Zn (values are presented as mean ± SD; n = 10); (c-,d) change in mass denotes specimens' biodegradation after incubation in SBF+LYS (values are presented as mean ± SD, n = 10); (e) change in mass denotes specimens' biodegradation after storage in SBF+Zn (values are mean ± SD, n = 10). (f) Amount of HYP released from constructs into SBF+Zn denotes degradation of the collagen component after their incubation in SBF+Zn (values are presented as mean ± SD, n = 10). Asterisks indicate statistical differences of pairwise groups, with *p = 0.01; **p < 0.01; ***p = 0.005; ****p < 0.001.

3.2. Sol−Gel Fraction Analysis. The analysis of sol (unreacted) monomer and gel (polymer) fractions showed that the structure of dentin ECM/Chitosan hydrogel constructs was, on average, 17% sol and 83% gel fraction. This indicates that the polymer structure in the thermoset freeze-dried hydrogel constructs was mostly well cross-linked.

3.3. Degree of Porosity and Morphology. The porosity analysis measured by liquid (ethanol) displacement showed that freeze-dried specimens of the dentin ECM hydrogel presented an average porosity ratio of 51.5 ± 2%. Surface morphology and porosity features of dentin ECM/Chitosan constructs are shown in Figure 3 panels.

SEM analyses conducted on either air-, chemical- (liquid CO_2 /critical point), or freeze-dried samples showed distinct morphological characteristics (Figure 3a−i). Samples that were air- or chemically dried shrank remarkably after the drying process (i.e., 30% and 20%, respectively), exhibiting a flake-like appearance with no distinctive evidence of regular porosities (Figure 3a−f). On the contrary, freeze-dried hydrogels exhibited minor or negligible overall shrinkage (0−3%) (Figure 3g−i) and an expressive number of well-defined pores with diameters varying from 15 to 95 μm (Figure 3j).

3.4. Water Sorption (WS), Solubility (SL), and Swelling Degree (d-SW). The effects of water storage in the hydrogel constructs, WS (mg/mm^3), SL (mg/mm^3), and d-SW (%), are summarized in Figure 4. Differences in WS were shown to be statistically significant between the second and eighth days and the second and 16th days of storage. No significant change in WS was found between the eighth and 16th days of storage (Figure 4a). The kinetics of water diffusion suggested that an equilibrium in WS values was reached between the eighth and 16th days of storage in water. While there was an increase in the SL values between 2 and 8 days of water storage, changes in SL values were not statistically significant among different storage times (Figure 4b). Likewise, the mean d-SW values varied slightly between the second and eighth days of storage, but no significant differences were found between endpoints (Figure 4c).

3.5. Modulus of Elasticity. The flexural modulus of elasticity (E) values for hydrogel-hydrated samples are depicted in Figure 5a,b. At the baseline, both sets of samples, stored in SBF+LYS or SBF+Zn, exhibited flexural E in the range of 3.47 (±0.64) and 3.89 (±0.85) MPa. No significant differences were found in baseline flexural E between the two groups.

For specimens challenged by storage in SBF+LYS, a significant decrease in flexural E values was noted for all tested time points compared to the corresponding baseline values (Figure 5a). Differences between storage time points were significant between 2- and 16-day storage (p < 0.01) and between 8- and 16-day storage (p = 0.001) (Figure 5a). The differences in flexural E for specimens stored in SBF+Zn were significant compared to the baseline for 8-day and 16-day endpoints. Differences between storage times for this set of specimens were significant only between 2- and 16 days of storage (Figure 5b).

3.6. Biodegradability. The biodegradability of hydrogel constructs is also depicted in Figure 5c−f. The gravimetric analyses denoted a reduction of the dry mass (mg) of specimens after incubation, regardless of whether the medium had been added with lysozyme or $ZnCl_2$. For samples stored in SBF+LYS, changes in dry mass compared to baseline were significant for 8 and 16 days. Differences were also found between 2 and 16 days and between 8 and 16 days of storage (Figure 5c). Gravimetric analyses showed significant differences in dry mass compared to the baseline only for the group stored for 16 days in SBF+Zn (Figure 5d). The HYP assay conducted in SBF+Zn media

https://doi.org/10.1021/acsomega.4c09413
ACS Omega 2025, 10, 9210−9223

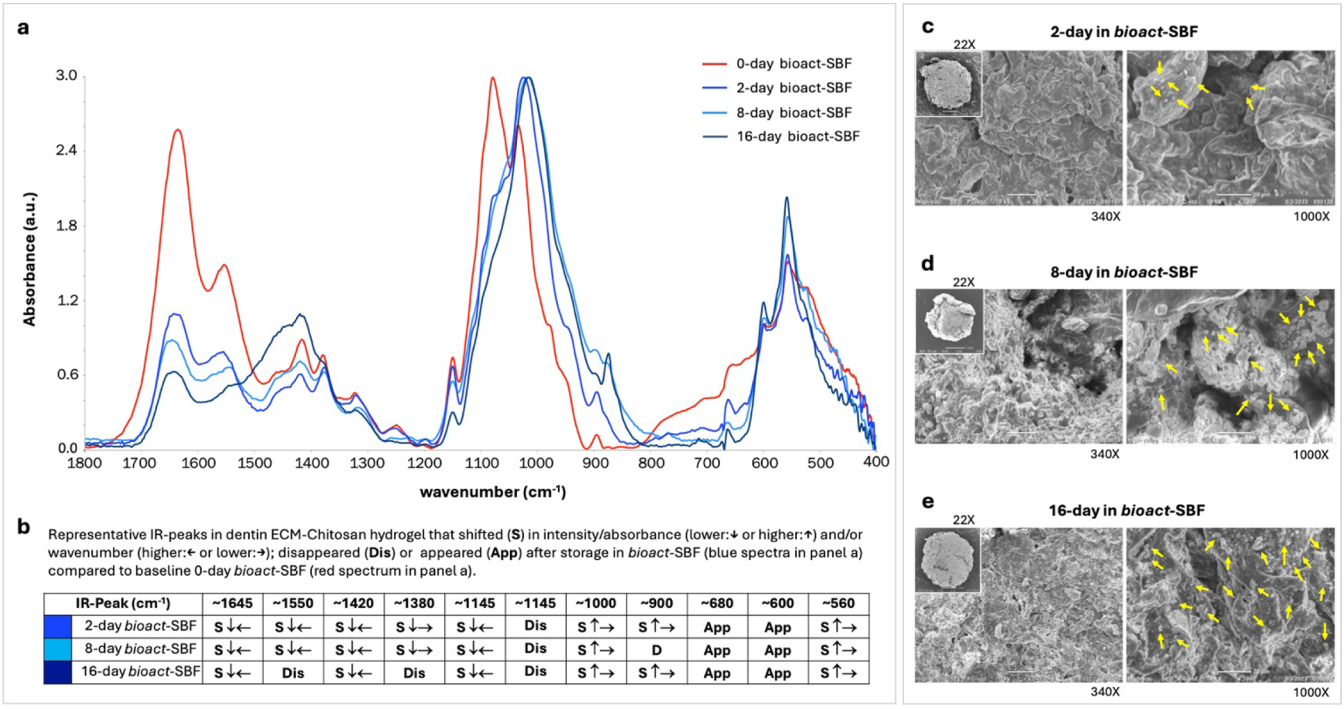

IR-Peak (cm-1)	~1645	~1550	~1420	~1380	~1145	~1145	~1000	~900	~680	~600	~560
2-day *bioact*-SBF	S↓←	S↓←	S↓←	S↓→	S↓←	Dis	S↑→	S↑→	App	App	S↑→
8-day *bioact*-SBF	S↓←	S↓←	S↓←	S↓→	S↓←	Dis	S↑→	D	App	App	S↑→
16-day *bioact*-SBF	S↓←	Dis	S↓←	Dis	S↓←	Dis	S↑→	S↑→	App	App	S↑→

Figure 6. FTIR and SEM analyses of representative dentin ECM/Chitosan hydrogel specimens tested for bioactivity while stored in bioact-SBF for 2, 8, or 16 days. (a,b) FTIR spectral analysis showed shifts (S) in the most evident peaks for samples incubated in bioact-SBF compared to baseline; as well as disappearance of baseline peaks (Dis) or appearance of new peaks (App). IR peaks corresponding to phosphate vibration (PO_4^3) of apatite at ~1000 cm^{-1} and ~560 cm^{-1} are shown at higher intensity and displaced toward a lower wavenumber for samples incubated in bioact-SBF. (c,d) SEM analysis of freeze-dried constructs (at 22×, 340×, and 1000× magnification) showed particles/deposits on specimens' surfaces (yellow arrows at 1000× magnification) suggesting the precipitation of apatite after storage in bioact-SBF for 2 (c), 8 (d), or 16 days (e).

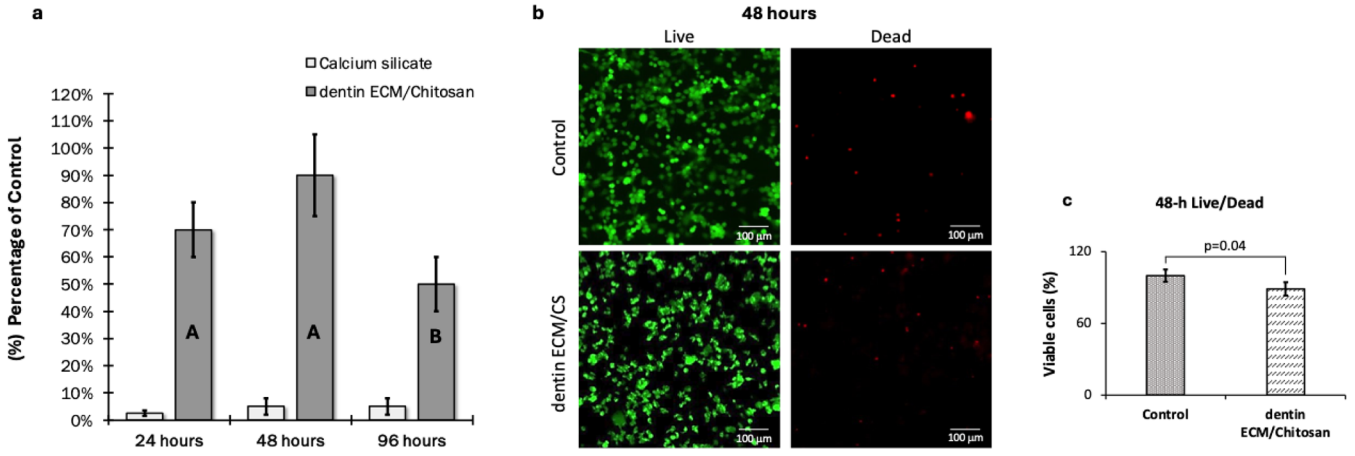

Figure 7. Biocompatibility of the dentin ECM/Chitosan hydrogel. (a) Alamar Blue assay. Values were expressed as percentage of control group (100% viability) ± SEM, which consisted of cells cultured directly on microplate wells. Viability of OD-21 cells seeded on hydrogel constructs was 70 ± 10% at 24 h, 90 ± 15% at 48 h, and 50 ± 35% at 96 h of experiments. Differences in cell viability in specimens of the hydrogel are depicted by different upper-case letters (with A > B; $p = 0.01$). Viability of OD-21 cells seeded on the calcium silicate biomaterial was significantly low throughout the experiments (2 to 5% of control). Pairwise comparison between calcium silicate (light gray bars) and the dentin ECM−Chitosan hydrogel (dark gray bars) at each time point showed statistical differences with $p < 0.001$. (b,c) Live/Dead assay. Representative fluorescence microscopy images of OD-21 cells acquired at green (live) and red channels (dead) depicted a slight difference in cells overall characteristics when cultured on the plate (control) or the developed hydrogel (dentin ECM/CS) (b). Values were expressed as percentage of control group (100% viability) ± SEM. Viability of OD-21 cells seeded on hydrogel constructs as assayed by the Live/Dead assay was 90 ± 10% at 48 h. Pairwise comparison between control and the dentin ECM/Chitosan hydrogel showed statistical differences with $p = 0.04$ (c). The viability of OD-21 cells in calcium silicate could not be assessed by the LIVE/DEAD kit (data not shown). $n = 3$ independent experiments/assay.

demonstrated a progressive elevation in the level of HYP as the time of storage increased (Figure 5e). Differences in collagen biodegradation (i.e., released HYP) were significant between all groups (Figure 5f).

3.7. In Vitro Bioactivity. ATR-FTIR spectra in Figure 6a show distinctive IR vibrational bands of dentin ECM/Chitosan constructs following incubation in bioact-SBF for 0 (baseline), 2, 8, or 16 days. Figure 6b depicts shifts and/or disappearance of

https://doi.org/10.1021/acsomega.4c09413
ACS Omega 2025, 10, 9210−9223

vibrational bands that are characteristic of the dentin ECM (NH_2, C═O, and −OH) and chitosan (NH_2 and −OH) in the wavenumber range of 950−1650 cm^{-1}. These IR spectral changes were observed since day 2 of immersion in bioact-SBF and followed by a significant increase up to day 16, which is considered a confirmation of in vitro hydrogel bioactivity.[21] In addition, the bioactive potential of the dentin ECM/Chitosan hydrogel is demonstrated by an increase in the intensity (higher arbitrary unit of absorbance) of peaks at ∼1000 cm^{-1} and at ∼560 cm^{-1} both corresponding to typical vibrations of PO_4^{3-} groups of apatite (Figure 6b), more likely the stretching asymmetric and symmetric vibrations of P−O bonds.[22,23]

The SEM qualitative analyses confirm that there was an exchange of ions between bioact-SBF and dentin ECM/Chitosan constructs, resulting in the deposition of precipitates on the surface of the hydrogel (Figure 6c−e). The number of precipitates seen on the hydrogel construct's surface was remarkably more abundant for samples incubated for longer in bioact-SBF.

3.8. Biocompatibility. The cell viability of OD-21 cells seeded on the dentin ECM/Chitosan hydrogel versus benchmark calcium silicate dental cement is shown in Figure 7a. The dentin ECM/Chitosan hydrogel exhibited significantly higher cell viability than the selected dental biomaterial when tested at 24, 48, and 96 h ($p < 0.05$). A significant increase in cell viability was detected for the dentin ECM/Chitosan hydrogel between 24- and 48-h incubation ($p < 0.01$) with survival rates of ∼70% and 90%, respectively, in relation to the control. After 96 h, OD-21 cells showed reduced viability, exhibiting approximately 50% cell survival and a large data variability, but still with higher cell survivability than the benchmark calcium silicate dental cement (Figure 7a).

Representative images from the LIVE/DEAD assay demonstrate no substantial difference between the appearance and distribution of OD-21 cells seeded directly into the microtiter plate well (control) and the cultured hydrogel specimens (Figure 7b). Furthermore, spectrophotometric analysis corroborated that at 48 h of cell culture, the dentin ECM/Chitosan hydrogel showed a 90% (±10) survival rate for OD-21 cells (Figure 7c) compared to the positive control considered as 100% viability (i.e., cells seeded directly onto the surface of the plate wells). The viability of OD-21 cells on calcium silicate could not be assessed by the LIVE/DEAD kit (data not shown).

4. DISCUSSION

There has been increasing interest in using isolated ECM components from native tissues to produce biomaterials, bioinks, and scaffolds for the endogenous regeneration of injured alike tissues. The major advantage of this tissue engineering approach is to employ three-dimensional analogs that mimic the biophysics and recapitulate the microenvironment of the tissue requiring regeneration. Currently, the reengineering of injured dental tissues is critically limited by the difficulty of obtaining adequate conditions for the proliferation and differentiation of dental pulp stem cells that, at the same time, allow an adequate blood supply to ensure endogenous tissue repair. The dentin ECM is a complex, porous, three-dimensional collagen-based matrix intermeshed with other macromolecules of relevant biological value (e.g., glycoproteins, growth factors, glycosaminoglycans, proteoglycans, among others).[11,12] Our primary hypothesis is that biomaterials derived from the dentin ECM would offer a holistic approach to aid regenerative therapies of dental tissues. Thus, the present study proposed the development of an injectable hydrogel that combines soluble and insoluble fractions of the dentin ECM with low molecular weight chitosan (50 000−190 000 Da).

The rationale for using chitosan to functionalize the dentin ECM stems not only from its own similarity to tissue ECM components (i.e., carbohydrates) but also from its demonstrated affinity to bind collagen,[33] the most abundant protein in the dentin ECM. In addition to possessing a myriad of biological properties, chitosan exhibits versatility to be processed into different forms (i.e., solutions, sponges, films, gel, paste, tablets, microspheres, microparticles, etc.), thus exhibiting enormous potential for use in biomedical applications. Several injectable/printable chitosan-collagen-based biomaterials have shown promising results in tissue regenerative schemes.[35−38] However, to our knowledge, this is the first study that designed and characterized an injectable thermosensitive hydrogel made by cross-linking chitosan with the dentin ECM.

The proposed hydrogel was optimized to be extrudable at room temperature and achieve thermosetting gelation at 37 °C. The concentrations of β-glycerol phosphate (BGP), pH, and temperature played important roles in achieving gelation and cross-linking of the hydrogel. It was suggested that interactions such as electrostatic attractions, repulsions, and ionic, hydrogen, and hydrophobic bonds are all involved in the physical gelation process of chitosan-BGP systems. Chitosan is insoluble in neutral and basic solutions but is soluble at a pK_a of 6.5 due to the protonation of free amino groups in its structure.[39] Titration of chitosan-based solutions to a pH between 6.2 and 6.5 results in the formation of a gel-like hydrated precipitate as the temperature is increased to a physiological range (≥37 °C). Consequently, it is inferred that temperature induces proton transfer between the anionic phosphate group of BGP and the cationic amine group in chitosan, leading to gel formation.[39]

We suspect that the mechanism of dentin ECM and chitosan gelation in the presence of BGP is also dependent on changes in pH and temperature. When pH is nearly neutral, collagen type I molecules are negatively charged and, therefore, compete for NH^{3+} of chitosan against BGP. At the same time, the addition of BGP into the acid-solubilized collagen/chitosan mixture leads to a pH increase in the system, which also allows for the self-assembly of collagen molecules to form insoluble fibrils/fibers.[39] For the preparation of the prehydrogel, we suspended the dentin ECM, and thereby collagen type I, in acetic acid. Thus, we assume the basic BGP solution served to neutralize the dentin ECM suspension, which, in combination with increased temperature, caused dentin collagen fibrillogenesis and gel formation.[39] While the mechanism of gel formation in the dentin ECM/Chitosan hydrogel has yet to be elucidated, it is exciting to envision that this novel biomaterial can be used to fill irregular-sized defects in decayed teeth or bone and achieve a high degree of cross-linking at body temperature within a clinically relevant time frame.

The injectability experiments using the prefilled syringe model allowed us to evaluate the rheological characteristics of the dentin ECM/Chitosan hydrogel. Compared to water, the developed hydrogel demonstrated flow behavior that is not exactly that of a Newtonian fluid.[25,26] Furthermore, although it was not directly evaluated, the viscosity of the dentin ECM/Chitosan hydrogel was estimated considering the hydrodynamic injection force and the friction force.[26] Injectability experiments are particularly important when considering the application of fluids and drugs that must pass through biological barriers and/

https://doi.org/10.1021/acsomega.4c09413
ACS Omega 2025, 10, 9210−9223

or tissue to be deposited at the desired site. It is worth noting that the proposed hydrogel was designed primarily to support tissue regeneration of the dentin-pulp complex of injured teeth and that its application at the site of the injury by injection would be direct, not being interposed by any biological/tissue barrier. In this sense, this material would be injected into the injured tooth, like any other dental restorative material. Thus, the fact that three-dimensional specimens of this hydrogel were constructed using pipettes (P-20 and P-1000) and a syringe/needle assembly by several operators (i.e., 5 coauthors in this manuscript) is a practical demonstration of the injectability of the hydrogel for its primary intended purpose.

The ATR-FTIR spectral analyses confirmed that the integration of the ECM of dentin and chitosan was successfully mediated by BGP. Changes in the typical vibrational bands of the dentin ECM (amides A, I, II, and III) strongly suggest that chitosan might have bound to the dentin ECM through intermolecular interactions with dentin type I collagen functional groups (amide groups at ∼3560−3000 cm^{-1}, ∼1658 cm^{-1}, and ∼1571 cm^{-1} and the −CH bending group at ∼1410 cm^{-1}).[41] It should be noted that the prominent peak observed at bands ∼1550−1571 cm^{-1} can be attributed to increased signaling of amide II upon interactions between the amino group of chitosan and the carbonyl groups of collagen type I.[21] Since type I collagen is the most abundant (∼90%) insoluble component of the dentin ECM, we assume it has likely been the dentin protein most highly modified by chitosan.

Moreover, it is expected that chitosan can further exhibit binding affinity for the functional groups of other dentin matrix macromolecules such as proteoglycans (i.e., amide groups of protein cores at ∼1571 cm^{-1} and vibrations of saccharide groups such as −CO stretching at ∼1080 cm^{-1}), glycosaminoglycans (i.e., vibration of the planar group −COO symmetric at ∼1410 cm^{-1} and saccharide vibrations assigned to −C−O−C bridge asymmetric stretching and −CO stretching at ∼1190 and 1080 cm^{-1}, respectively), and residual apatite (i.e., vibrations of carbonate at ∼1070 cm^{-1} and phosphate groups at ∼1000 cm^{-1} and in the range of 650−500 cm^{-1}).[41−43]

The densely interconnected structure observed in freeze-dried dentin ECM/Chitosan endorses the notion of successful hybridization of raw components in the developed hydrogel (Figure 3g−j), providing further insight into its micro-architecture, degree of porosity, and morphological features, which are important parameters for cell infiltration and survival. It has been shown that porosity features (i.e., number, distribution, diameter, and geometry) can significantly contribute to both the conductive properties of hydrogel constructs and the functionality of embedded cells.[44] Since pores in hydrogel-based scaffolds allow for nutrient flow and supply, they are considered pivotal for cell adhesion, ingrowth, proliferation, and migration, thus playing a key role in tissue growth and regeneration.[45,46]

As essential as the presence of microsized pores, the physical and mechanical properties of scaffolds are also key to providing cues for cell survivability and proliferation. The polymer matrix of dentin ECM/Chitosan constructs was found to be well cross-linked as estimated by the sol−gel fraction of 83% polymers formed. Accordingly, such a relatively high degree of cross-linking had a marked influence on ECM/Chitosan constructs' behavior in response to water diffusion, mechanical properties, and in vitro biodegradability.

The ability to absorb water and form swollen networks provides scaffolds with an additional means to accommodate the transit and diffusion of molecules and cells. At the same time, undergoing excessive fluid sorption may significantly affect polymeric scaffolds' dimensional and mechanical stability.[47] Thus, the assessment of hydrogels' water sorption (WS), solubility (SL), and degree of swelling (d-SW) is important to determine their scaffolding features.[28] WS and SL values were higher for dentin ECM/Chitosan constructs stored for prolonged periods (i.e., 8 or 16 days). However, no significant changes in WS or SL were observed between samples stored in water for 8 and 16 days. This suggests that the kinetics of water diffusion have likely found an equilibrium during the first days of storage in water.

Surprisingly, the degree of swelling (d-SW), which determined the extent of volumetric changes in freeze-dried constructs of the dentin ECM/Chitosan hydrogel, did not vary as a function of the water storage time. This corroborates the assumption that water diffusion and subsequent desorption and leaching of unreacted components from the hydrogel constructs must have reached a dynamic balance within the first days or perhaps hours of storage in water. Moreover, the d-SW experiment suggests a relative stability of the dentin ECM/Chitosan hydrogel, at least when stored in water for up to 16 days. Future studies will be conducted to determine the diffusion kinetics of water and other solvents (i.e., PBS, cell culture media) in specimens of dentin ECM/Chitosan following the first 24 h of storage.

Specificities underlying the phenomena of hydration (imbibition) and dehydration (syneresis) in hydrogels are intrinsically related to the polymer composition, hydrophilicity, and structural arrangement.[47] The water diffusion pattern and resultant swelling and solubility are greatly affected by the degree of polymer cross-linking and the balance between the macromolecular packing density and effective free volume within the hydrogel.[48] Thus, we speculate that a high degree of polymer cross-linking has somehow limited the ability of dentin ECM/Chitosan constructs to swell and leach out unreacted components, regardless of the period of time they remained stored in water.

A fundamental intention of this study was to formulate a biomaterial that could replicate the mechanical behavior of the tissue to be reengineered (e.g., dentin, dental pulp, and eventually dental alveolar bone). Here, the three-point bending test was selected because, among all the standardized mechanical configurations in our laboratory, including compression and tension, this is the only method that allows a nondestructive evaluation of the samples. Furthermore, the three-point bending test offers good control to select between stress and strain ranges within the elastic deformation of the material, providing means for the calculation of the true flexural modulus of elasticity. Dentin ECM/Chitosan bar-like constructs exhibited a flexural elastic modulus on a scale of MPa, with values ranging between 3.5 and 4.5 MPa. Notably, these values are in the same order of magnitude as demineralized dentin specimens of similar geometry and dimensions that have been tested in our laboratory in the past under the same hydration conditions (e.g., immersed in water) and similar temperature and relative humidity parameters.[30,32] Other chitosan-collagen hydrogels have been reported to exhibit flexural and/or compressive elastic moduli in the range of KPa,[37−50] which represents a difference in stiffness of approximately 1000 times smaller compared to the dentin ECM/Chitosan hydrogel presented here. It is reassuring to find that our newly developed hydrogel may be effectively more suitable for re-engineering

https://doi.org/10.1021/acsomega.4c09413
ACS Omega 2025, 10, 9210−9223

injured load-bearing dental tissues than currently available collagen-chitosan-based biomaterials.

The endurance of hydrogels' mechanical performance also depends on polymer structural parameters such as their composition, degree of cross-linking, porosity features (i.e., pore size, density, and distribution), and balance between polymer chain packing and free volume ratios.[21,50] Overall, incubation in SBF with lysozyme or $ZnCl_2$ demonstrated a detrimental impact on the elastic modulus of the dentin ECM/Chitosan hydrogel, with a reduction in flexural *E* values being notably more significant for specimens incubated in SBF containing lysozyme. As mentioned previously, lysozyme was chosen to challenge the degradability of the hydrogel specimens by cleavage of chitosan glycosidic bonds,[29,32] whereas SBF added with Zn was intended to accelerate dentin collagen hydrolysis by activation of endogenous dentin matrix metalloproteases.[31,33] As the most predominant component in the present hydrogel is chitosan, it was expected to detect a higher biodegradation rate in specimens stored in SBF containing lysozyme, which was actually confirmed.

In addition to the loss of mechanical competence, gravimetric analysis indicated that the constructs of dentin ECM/Chitosan stored in SBF+LYS also showed greater mass loss. Thus, altogether, the reduction in flexural *E* and greater mass loss suggest that the breakdown of *N*-acetylmuramic acid-*N*-acetyl-D-glucosamine linkages in chitosan contributed the most to the biodegradation of the dentin ECM/Chitosan hydrogel. Here, again, these results seem to be coherent, considering the high concentration of chitosan (75%) in this biomaterial.

The in vitro bioactivity of dentin ECM/Chitosan constructs highlights an important biological attribute of the newly developed hydrogel. According to the classic definition, bioactivity refers to the capacity of a biomaterial to promote the biomineralization of natural tissues by the formation of calcium phosphate deposits following exposure to a body fluid.[22,23] It is worth noting that the SBF used in the present in vitro bioactivity study was formulated to have an ionic concentration equivalent to that of human blood plasma.[30,34] The SEM analysis distinctly showed that an ion exchange between the SBF and the hydrogel led to the nucleation of crystal-like deposits on the hydrogel surface. This was observed as early as day 2 of incubation and increased progressively as the time of incubation in SBF was extended to 16 days.

The FTIR spectral analysis strongly validates the bioactive properties of the dentin ECM/Chitosan hydrogel. Vibrational peaks corresponding to the functional groups of components of dentin ECM/Chitosan (in the wavenumber range of 1650−950 cm^{-1}) were modified or disappeared upon SBF incubation. A marked spectral change of the band at ∼1000−1030 toward ∼978−1018 cm^{-1} after incubation in SBF indicates the coincidence of symmetrical stretching vibration of C═O and P−O bonds typical of apatite mineral.[23] Moreover, the displacement of the peak from ∼560 cm^{-1} to 550 cm^{-1} and toward a higher absorbance also points to the presence of IR vibrations corresponding to PO_4^{3-} groups typically found in apatite.[21]

As previously conjectured, such in vitro nucleation of apatite deposits on dentin ECM/Chitosan construct surfaces might have been likely prompted by reactions between anionic and cationic groups such as −COO, −OH, C═O, and $-NH_2$ in the hydrogel.[51] Accordingly, these positively and negatively charged groups would act as active sites for calcium and phosphate ions to form complexes and lead to apatite precipitation onto the samples' surface. These exciting findings encourage us to assume that the ability of apatite to form in a relatively short period of time on the surface of dentin ECM/Chitosan in SBF anticipates the in vivo bioactivity potential of this new biomaterial.

As the proposed hybrid hydrogel holds properties of its raw constituents, it was expected to provide an appropriate microenvironment for cell survival and proliferation. As a proof of concept, we used an in vitro model to assess the biocompatibility of a newly developed hydrogel. Taking into consideration all limitations inherent to in vitro models, we found that OD-21 mice undifferentiated pulp cells exhibited survival rates of 70% and 90% relative to control, respectively, at 24 and 48 h of culture. After 96 h, OD-21 cells showed reduced viability, including in the control group (cells cultured directly on plate wells), and their survival rate in hydrogel constructs was approximately 50%, showing no significant change at 168 h (i.e., 1 week), when cell culture experiments were completed (data not shown). These results can be partly credited to the lack of cell-specific adhesion binding sites in the hydrogel,[9] but also to the space constraints imposed by the small wells of the 96-well microplates, which after a week of culture also interfered with the growth and proliferation of positive control OD-21 cells. We speculate that once cells are encapsulated in the hybrid hydrogel and cell proliferation rates are estimated using a three-dimensional positive control (e.g., collagen or gelatin constructs), it will be possible to detect an ascendant course in cell survival and proliferation.

The LIVE/DEAD viability/cytotoxicity assay confirmed the high biocompatibility of the dentin ECM/Chitosan hydrogel at 48 h of analysis, indicating an average survival rate of 90% compared with the positive control. Furthermore, representative fluorescence images demonstrated that the overall morphological characteristics of OD-21 cells seeded on the hydrogel surface were not remarkably different from those of the control, in which the cells were cultured directly on the well plate surface. While we recognize that these in vitro results are inherently limited, it is encouraging to know that the developed hydrogel demonstrates negligible cytotoxicity.

We understand the limitations of the present study and acknowledge the need to conduct in vivo experiments to validate the safety and effectiveness of the proposed hydrogel in a physiological environment. In addition, we have been studying the effect of other ratios of base components, dentin ECM, and chitosan. The development and applicability of this new biomaterial will depend on future studies, with two potential approaches being explored. The first and perhaps ideal strategy would rely on cells derived from patients themselves, thereby ensuring compatibility and reducing the risk of rejection. Accordingly, the fresh prehydrogel would be injected in situ into the injured tissue to provide conditions for resident stem cells to proliferate, differentiate, and subsequently allow for tissue regeneration utilizing local blood supply and growth factors derived from hydrogel biodegradation. Alternatively, if it is deemed suitable through further investigations, the hydrogel can be loaded with human-extracted stem cells, which would be delivered to fill defective tissue by extrusion. This hydrogel formulation would be designed to provide a controlled release of bioactive agents, promoting tissue regeneration and healing without the need for additional cell-based interventions. We envision that the determination of the most appropriate strategy will depend on forthcoming research and scientific advancements in the field.

https://doi.org/10.1021/acsomega.4c09413
ACS Omega 2025, 10, 9210−9223

5. CONCLUSIONS

Smart biomaterials are defined as being capable of sensing physiological and microenvironmental oscillations in pH, temperature, ionic strength, mechanical stress, and/or the influx of bioactive molecules and, as a consequence, adapting their responses to modulate their own biological effects. Considering this definition, we may conclude that the newly developed dentin ECM/Chitosan biomaterial is a smart hydrogel. Morphological, physical, mechanical, and biocompatibility features of this novel biomaterial suggest it could serve as a cell-inductive scaffold, which obviously needs to be confirmed in future studies using animal models. The thermoresponsive, injectable, and bioactive properties of the proposed hydrogel offer promising perspectives for its use as a minimally invasive and biocompatible scaffold in dental and medical tissue engineering applications.

AUTHOR INFORMATION

Corresponding Author

Marcela R. Carrilho − *College of Dental Medicine-Illinois, Midwestern University, Downers Grove, Illinois 60515, United States;* orcid.org/0000-0002-7171-6108; Phone: + 1 630-515-7237; Email: mcarri@midwestern.edu

Authors

Sajdah Arbeed − *College of Graduate Studies-Illinois, Midwestern University, Downers Grove, Illinois 60515, United States*

Maya Osman − *College of Graduate Studies-Illinois, Midwestern University, Downers Grove, Illinois 60515, United States*

Feng Gao − *College of Dental Medicine-Illinois, Midwestern University, Downers Grove, Illinois 60515, United States*

Stephen Suchy − *College of Dental Medicine-Illinois, Midwestern University, Downers Grove, Illinois 60515, United States*

Zinat Sharmin − *College of Dental Medicine-Illinois, Midwestern University, Downers Grove, Illinois 60515, United States*

Joshua Z. Gasiorowski − *College of Graduate Studies-Illinois, Midwestern University, Downers Grove, Illinois 60515, United States*

Amber Kaminski − *College of Graduate Studies-Illinois, Midwestern University, Downers Grove, Illinois 60515, United States;* orcid.org/0000-0003-4181-2972

Ira M. Sigar − *College of Graduate Studies-Illinois, Midwestern University, Downers Grove, Illinois 60515, United States*

Complete contact information is available at: https://pubs.acs.org/10.1021/acsomega.4c09413

Funding

This study was supported by the MWU intramural grant/Biomedical Sciences Master Program (Sajdah Arbeed) and the NIH/NIDCR grant R15DE032836 (P.I. Marcela R. Carrilho).

Notes

The authors declare no competing financial interest.

ACKNOWLEDGMENTS

This research was part of the requisites for a Master of Biomedical Sciences thesis by Sajdah Arbeed at MWU-IL. All the experiments presented in the manuscript were conducted, optimized, and repeated at least 3 times for consistency within a period of 10 months. The authors thank the scientific advice provided by Dr. John C. Mitchell and the instrumental technical support of Drs. Bhimanna Kuppast, Ellen Kohlmeir, and Shridhar Andurkar, as well as MWU-IL Pharmaceutical Sciences and MWU-IL Core Facilities.

REFERENCES

(1) Zhang, W.; Yelick, P. C. Craniofacial Tissue Engineering. *Cold Spring Harb. Perspect. Med.* **2018**, *8*, a025775.

(2) Zhao, F.; Zhang, Z.; Guo, W. 2024. The 3-dimensional printing for dental tissue regeneration: the state of the art and future challenges. *Front. Bioeng. Biotechnol.* **2024**, *12*, 1356580.

(3) Dubey, N.; Ferreira, J. A.; Malda, J.; Bhaduri, S. B.; Bottino, M. C. Extracellular Matrix/Amorphous Magnesium Phosphate Bioink for 3D Bioprinting of Craniomaxillofacial Bone Tissue. *ACS Appl. Mater. Interfaces* **2020**, *12*, 23752−23763.

(4) Li, M.; Sun, D.; Zhang, J.; Wang, Y.; Wei, Q.; Wang, Y. Application and development of 3D bioprinting in cartilage tissue engineering. *Biomater. Sci.* **2022**, *10*, 5430−5458.

(5) Cruz Walma, D. A.; Yamada, K. M. Extracellular Matrix in Human Craniofacial Development. *J. Dent. Res.* **2022**, *101*, 495−504.

(6) Liu, C.; Pei, M.; Li, Q.; Zhang, Y. Decellularized extracellular matrix mediates tissue construction and regeneration. *Front. Med.* **2022**, *16*, 56−82.

(7) Conway, J. R. W.; Isomursu, A.; Follain, G.; Härmä, V.; Jou-Ollé, E.; Pasquier, N.; Välimäki, E. P. O.; Rantala, J. K.; Ivaska, J. Defined extracellular matrix compositions support stiffness-insensitive cell spreading and adhesion signaling. *Proc. Natl. Acad. Sci. U.S.A.* **2023**, *120*, No. e2304288120.

(8) Zheng, C. X.; Sui, B. D.; Hu, C. H.; Qiu, X. Y.; Zhao, P.; Jin, Y. Reconstruction of structure and function in tissue engineering of solid organs: Toward simulation of natural development based on decellularization. *J. Tissue Eng. Regen Med.* **2018**, *12*, 1432−1447.

(9) Athirasala, A.; Tahayeri, A.; Thrivikraman, G.; França, C. M.; Monteiro, N.; Tran, V.; Ferracane, J.; Bertassoni, L. E. A dentin-derived hydrogel bioink for 3D bioprinting of cell laden scaffolds for regenerative dentistry. *Biofabrication* **2018**, *10*, 024101.

(10) Zhang, C. Y.; Fu, C. P.; Li, X. Y.; Lu, X. C.; Hu, L. G.; Kankala, R. K.; Wang, S. B.; Chen, A. Z. Three-Dimensional Bioprinting of Decellularized Extracellular Matrix-Based Bioinks for Tissue Engineering. *Molecules* **2022**, *27*, 3442.

(11) Bertassoni, L. E. Dentin on the nanoscale: Hierarchical organization, mechanical behavior and bioinspired engineering. *Dent. Mater.* **2017**, *33*, 637−649.

(12) Desoutter, A.; Felbacq, D.; Gergely, C.; Varga, B.; Bonnet, L.; Etienne, P.; Vialla, R.; Cuisinier, F.; Salehi, H.; Rousseau, E.; Rufflé, B. Properties of dentin, enamel and their junction, studied with Brillouin scattering and compared to Raman microscopy. *Arch. Oral Biol.* **2023**, *152*, 105733.

(13) Alia, A. *Development of Dentin-Derived Hydrogels*. Master thesis.; Midwestern University, Biomedical Sciences: Downers Grove, IL, USA, 2021.

(14) Aguilar, A.; Zein, N.; Harmouch, E.; Hafdi, B.; Bornert, F.; Offner, D.; Clauss, F.; Fioretti, F.; Huck, O.; Benkirane-Jessel, N.; Hua, G. Application of Chitosan in Bone and Dental Engineering. *Molecules* **2019**, *24*, 3009.

(15) Kou, S. G.; Peters, L. M.; Mucalo, M. R. Chitosan: A review of sources and preparation methods. *Int. J. Biol. Macromol.* **2021**, *169*, 85−94.

(16) Zhang, C.; Hui, D.; Du, C.; Sun, H.; Peng, W.; Pu, X.; Li, Z.; Sun, J.; Zhou, C. Preparation and application of chitosan biomaterials in dentistry. *Int. J. Biol. Macromol.* **2021**, *167*, 1198−1210.

(17) Salehi, S.; Cooper, P.; Smith, A.; Ferracane, J. Dentin matrix components extracted with phosphoric acid enhance cell proliferation and mineralization. *Dent. Mater.* **2016**, *32*, 334−342.

(18) Reis, M.; Alania, Y.; Leme-Kraus, A.; Free, R.; Joester, D.; Ma, W.; Irving, T.; Bedran-Russo, A. K. The stoic tooth root: how the

mineral and extracellular matrix counterbalance to keep aged dentin stable. *Acta Biomater.* **2022**, *138*, 351−360.
(19) Carrilho, M. R.; Scaffa, P. M. C.; Dionizio, A.; Ventura, T. M. O.; Buzalaf, M. A. R.; Vidal, C. M. P. Differential analysis of the dentin soluble proteomic. *J. Dent.* **2023**, *131*, 104454.
(20) Chen, J.; Sun, T.; Lin, B.; Wu, B.; Wu, J. The Essential Role of Proteoglycans and Glycosaminoglycans in Odontogenesis. *J. Dent. Res.* **2024**, *103*, 345−358.
(21) Kaur, K.; Paiva, S. S.; Caffrey, D.; Cavanagh, B. L.; Murphy, C. M. Injectable chitosan/collagen hydrogels nano-engineered with functionalized single wall carbon nanotubes for minimally invasive applications in bone. *Mater. Sci. Eng.: C* **2021**, *128*, 112340.
(22) Dang, Q.; Liu, K.; Zhang, Z.; Liu, C.; Liu, X.; Xin, Y.; Cheng, X.; Xu, T.; Cha, D.; Fan, B. Fabrication and evaluation of thermosensitive chitosan/collagen/α, β-glycerophosphate hydrogels for tissue regeneration. *Carbohydr. Polym.* **2017**, *167*, 145−157.
(23) Rahmanian-Devin, P.; Baradaran Rahimi, V.; Askari, V. R. Thermosensitive Chitosan-beta-Glycerophosphate Hydrogels as Targeted Drug Delivery Systems: An Overview on Preparation and Their Applications. *Adv. Pharmacol. Pharm. Sci.* **2021**, *2021*, 6640893.
(24) Osmond, M. J.; Krebs, M. D. Tunable chitosan-calcium phosphate composites as cell-instructive dental pulp capping agents. *J. Biomater. Sci., Polym. Ed.* **2021**, *32*, 1450−1465.
(25) Allmendinger, A.; Fischer, S.; Huwyler, J.; Mahler, H. C.; Schwarb, E.; Zarraga, I. E.; Mueller, R. Rheological characterization and injection forces of concentrated protein formulations: an alternative predictive model for non-Newtonian solutions. *Eur. J. Pharm. Biopharm.* **2014**, *87*, 318−328.
(26) Wu, L.; Li, H.; Wang, Y.; Liu, C.; Zhao, Z.; Zhuang, G.; Chen, Q.; Zhou, W.; Guo, J. Advancing injection force modeling and viscosity-dependent injectability evaluation for prefilled syringes. *Eur. J. Pharm. Biopharm.* **2024**, *197*, 114221.
(27) Qin, H.; Wang, J.; Wang, T.; Gao, X.; Wan, Q.; Pei, X. Preparation and Characterization of Chitosan/beta-Glycerophosphate Thermal-Sensitive Hydrogel Reinforced by Graphene Oxide. *Front. Chem.* **2018**, *6*, 565.
(28) Ahmad, U.; Sohail, M.; Ahmad, M.; Minhas, M. U.; Khan, S.; Hussain, Z.; Kousar, M.; Mohsin, S.; Abbasi, M.; Shah, S. A.; Rashid, H. Chitosan based thermosensitive injectable hydrogels for controlled delivery of loxoprofen: development, characterization and in-vivo evaluation. *Int. J. Biol. Macromol.* **2019**, *129*, 233−245.
(29) Caballero-Flores, H.; Nabeshima, C. K.; Sarra, G.; Moreira, M. S.; Arana-Chavez, V. E.; Marques, M. M.; Machado, M. E. L. Development and characterization of a new chitosan-based scaffold associated with gelatin, microparticulate dentin and genipin for endodontic regeneration. *Dent. Mater.* **2021**, *37*, No. e414−e425.
(30) Kokubo, T.; Yamaguchi, S. Simulated body fluid and the novel bioactive materials derived from it. *J. Biomed Mater. Res. A* **2019**, *107*, 968−977.
(31) Omar, H.; Gao, F.; Yoo, H.; Bim Jr, O.; Garcia, C.; LePard, K. J.; Mitchell, J. C.; Agostini-Walesch, G.; Carrilho, M. R. Changes to dentin extracellular matrix following treatment with plant-based polyphenols. *J. Mech. Behav. Biomed. Mater.* **2022**, *126*, 105055.
(32) Kim, S.; Cui, Z. K.; Koo, B.; Zheng, J.; Aghaloo, T.; Lee, M. Chitosan-Lysozyme Conjugates for Enzyme-Triggered Hydrogel Degradation in Tissue Engineering Applications. *ACS Appl. Mater. Interfaces* **2018**, *10*, 41138−41145.
(33) Yoo, H.; Gao, F.; Agostini-Walesch, G.; Alabsy, M.; Mitchell, J. C.; Carrilho, M. R. Use of marine occurrent extracts to enhance the stability of dentin extracellular matrix. *J. Mech. Behav. Biomed. Mater.* **2024**, *154*, 106498.
(34) Baino, F.; Yamaguchi, S. The Use of Simulated Body Fluid (SBF) for Assessing Materials Bioactivity in the Context of Tissue Engineering: Review and Challenges. *Biomimetics* **2020**, *5*, 57.
(35) Itai, S.; Suzuki, K.; Kurashina, Y.; Kimura, H.; Amemiya, T.; Sato, K.; Nakamura, M.; Onoe, H. Cell-encapsulated chitosan-collagen hydrogel hybrid nerve guidance conduit for peripheral nerve regeneration. *Biomed. Microdevices* **2020**, *22*, 81.
(36) Arpornmaeklong, P.; Sareethammanuwat, M.; Apinyauppatham, K.; Boonyuen, S. Characteristics and biologic effects of thermosensitive quercetin-chitosan/collagen hydrogel on human periodontal ligament stem cells. *J. Biomed Mater. Res. B Appl. Biomater.* **2021**, *109*, 1656−1670.
(37) Liu, Y.; Luo, X.; Wu, W.; Zhang, A.; Lu, B.; Zhang, T.; Kong, M. Dual cure (thermal/photo) composite hydrogel derived from chitosan/collagen for in situ 3D bioprinting. *Int. J. Biol. Macromol.* **2021**, *182*, 689.
(38) Ohmes, J.; Saure, L. M.; Schütt, F.; Trenkel, M.; Seekamp, A.; Scherließ, R.; Adelung, R.; Fuchs, S. Injectable Thermosensitive Chitosan-Collagen Hydrogel as A Delivery System for Marine Polysaccharide Fucoidan. *Mar. Drugs* **2022**, *20*, 402.
(39) Saravanan, S.; Vimalraj, S.; Thanikaivelan, P.; Banudevi, S.; Manivasagam, G. A review on injectable chitosan/beta glycerophosphate hydrogels for bone tissue regeneration. *Int. J. Biol. Macromol.* **2019**, *121*, 38−54.
(40) Shan, J.; Tang, B.; Liu, L.; Sun, X.; Shi, W.; Yuan, T.; Liang, J.; Fan, Y.; Zhang, X. Development of chitosan/glycerophosphate/collagen thermo-sensitive hydrogel for endoscopic treatment of mucosectomy-induced ulcer. *Mater. Sci. Eng.: C* **2019**, *103*, 109870.
(41) Paschalis, E. P.; Gamsjaeger, S.; Klaushofer, K. Vibrational spectroscopic techniques to assess bone quality. *Osteoporos Int.* **2017**, *28*, 2275−2291.
(42) Rieppo, L.; Saarakkala, S.; Närhi, T.; Holopainen, J.; Lammi, M.; Helminen, H. J.; Jurvelin, J. S.; Rieppo, J. Quantitative analysis of spatial proteoglycan content in articular cartilage with Fourier transform infrared imaging spectroscopy: Critical evaluation of analysis methods and specificity of the parameters. *Microsc. Res. Technol.* **2010**, *73*, 503−512.
(43) Brézillon, S.; Untereiner, V.; Lovergne, L.; Tadeo, I.; Noguera, R.; Maquart, F. X.; Wegrowski, Y.; Sockalingum, G. D. Glycosaminoglycan profiling in different cell types using infrared spectroscopy and imaging. *Anal. Bioanal. Chem.* **2014**, *406*, 5795−5803.
(44) Omidian, H.; Chowdhury, S. D.; Wilson, R. L. Advancements and Challenges in Hydrogel Engineering for Regenerative Medicine. *Gels* **2024**, *10*, 238.
(45) Werner, D.; Maier, J.; Kaube, N.; Geske, V.; Behnisch, T.; Ahlhelm, M.; Moritz, T.; Michaelis, A.; Gude, M. Tailoring of Hierarchical Porous Freeze Foam Structures. *Materials* **2022**, *15*, 836.
(46) López-García, S.; Aznar-Cervantes, S. D.; Pagán, A.; Llena, C.; Forner, L.; Sanz, J. L.; García-Bernal, D.; Sánchez-Bautista, S.; Ceballos, L.; et al. 3D Graphene/silk fibroin scaffolds enhance dental pulp stem cell osteo/odontogenic differentiation. *Dent. Mater.* **2024**, *40*, 431−440.
(47) Karoyo, A. H.; Wilson, L. D. A Review on the Design and Hydration Properties of Natural Polymer-Based Hydrogels. *Materials* **2021**, *14*, 1095.
(48) Axpe, E.; Chan, D.; Offeddu, G. S.; Chang, Y.; Merida, D.; Hernandez, H. L.; Appel, E. A. A Multiscale Model for Solute Diffusion in Hydrogels. *Macromolecules* **2019**, *52*, 6889−6897.
(49) Mousavi, S.; Khoshfetrat, A. B.; Khatami, N.; Ahmadian, M.; Rahbarghazi, R. Comparative study of collagen and gelatin in chitosan-based hydrogels for effective wound dressing: Physical properties and fibroblastic cell behavior. *Biochem. Biophys. Res. Commun.* **2019**, *518*, 625−631.
(50) Khodabakhsh Aghdam, S.; Khoshfetrat, A. B.; Rahbarghazi, R.; Jafarizadeh-Malmiri, H.; Khaksar, M. Collagen modulates functional activity of hepatic cells inside alginate-galactosylated chitosan hydrogel microcapsules. *Int. J. Biol. Macromol.* **2020**, *156*, 1270−1278.
(51) Kaynak Bayrak, G.; Demirtaş, T. T.; Gümüşderelioğlu, M. Microwave-induced biomimetic approach for hydroxyapatite coatings of chitosan scaffolds. *Carbohydr. Polym.* **2017**, *157*, 803−813.

https://doi.org/10.1021/acsomega.4c09413
ACS Omega 2025, 10, 9210−9223